Appendix 3

ACOUSTIC PLANE WAVE PROPERTIES

A. CHRISTOFFEL EQUATIONS FOR ISOTROPIC AND ANISOTROPIC SOLIDS†

ISOTROPIC AND CUBIC

$$k^2\begin{bmatrix} c_{11}l_x + c_{44}(1-l_x^2) & (c_{12}+c_{44})l_x l_y & (c_{12}+c_{44})l_x l_z \\ (c_{12}+c_{44})l_x l_y & c_{11}l_y^2 + c_{44}(1-l_y^2) & (c_{12}+c_{44})l_y l_z \\ (c_{12}+c_{44})l_x l_z & (c_{12}+c_{44})l_y l_z & c_{11}l_z^2 + c_{44}(1-l_z^2) \end{bmatrix}\begin{bmatrix} v_x \\ v_y \\ v_z \end{bmatrix} = \rho\omega^2\begin{bmatrix} v_x \\ v_y \\ v_z \end{bmatrix}$$

$c_{11} = c_{12} + 2c_{44}$ for the isotropic case.

† The wave vector *direction* is defined by the unit vector

$$\hat{\mathbf{l}} = \hat{\mathbf{x}}l_x + \hat{\mathbf{y}}l_y + \hat{\mathbf{z}}l_z$$

where the coordinate axes x, y, z coincide with the crystal axes X, Y, Z in Table 7.1.

HEXAGONAL

$$k^2\begin{bmatrix} c_{11}l_x^2 + c_{66}l_y^2 + c_{44}l_z^2 & (c_{12}+c_{66})l_xl_y & (c_{13}+c_{44})l_xl_z \\ (c_{12}+c_{66})l_xl_y & c_{66}l_x^2 + c_{11}l_y^2 + c_{44}l_z^2 & (c_{13}+c_{44})l_yl_z \\ (c_{13}+c_{44})l_xl_z & (c_{13}+c_{44})l_yl_z & c_{44}l_x^2 + c_{44}l_y^2 + c_{33}l_z^2 \end{bmatrix}\begin{bmatrix} v_x \\ v_y \\ v_z \end{bmatrix} = \rho\omega^2\begin{bmatrix} v_x \\ v_y \\ v_z \end{bmatrix}$$

$$c_{66} = \tfrac{1}{2}(c_{11} - c_{12}).$$

TRIGONAL

Classes 32, 3m, $\bar{3}m$

$$k^2\begin{bmatrix} c_{11}l_x^2 + c_{66}l_y^2 + c_{44}l_z^2 + 2c_{14}l_yl_z & (c_{12}+c_{66})l_xl_y + 2c_{14}l_xl_z & (c_{13}+c_{44})l_xl_z + 2c_{14}l_xl_y \\ (c_{12}+c_{66})l_xl_y + 2c_{14}l_xl_z & c_{66}l_x^2 + c_{11}l_y^2 + c_{44}l_z^2 - 2c_{14}l_yl_z & (c_{13}+c_{44})l_yl_z + c_{14}(l_x^2 - l_y^2) \\ (c_{13}+c_{44})l_xl_z + 2c_{14}l_xl_y & (c_{13}+c_{44})l_yl_z + c_{14}(l_x^2 - l_y^2) & c_{44}(l_x^2 + l_y^2) + c_{33}l_z^2 \end{bmatrix}$$

$$\times \begin{bmatrix} v_x \\ v_y \\ v_z \end{bmatrix} = \rho\omega^2\begin{bmatrix} v_x \\ v_y \\ v_z \end{bmatrix}$$

$$c_{66} = \tfrac{1}{2}(c_{11} - c_{12}).$$

Classes 3, $\bar{3}$. In 7.11 the elements of the Christoffel matrix are:

$$\alpha = c_{11}l_x^2 + c_{66}l_y^2 + c_{44}l_z^2 + 2c_{14}l_yl_z - 2c_{25}l_zl_x$$
$$\beta = c_{66}l_x^2 + c_{11}l_y^2 + c_{44}l_z^2 - 2c_{14}l_yl_z + 2c_{25}l_zl_x$$
$$\gamma = c_{44}(l_x^2 + l_y^2) + c_{33}l_z^2$$
$$\delta = (c_{12}+c_{66})l_xl_y + 2c_{14}l_zl_x + 2c_{25}l_yl_z$$
$$\epsilon = -c_{25}(l_x^2 - l_y^2) + (c_{13}+c_{44})l_zl_x + 2c_{14}l_xl_y$$
$$\zeta = c_{14}(l_x^2 - l_y^2) + (c_{13}+c_{44})l_yl_z + 2c_{25}l_xl_z.$$

TETRAGONAL

Classes 4mm, 422, $\bar{4}2m$, 4/mmm. Same as hexagonal, but with arbitrary c_{66}.

Classes 4, $\bar{4}$, 4/m

$$k^2\begin{bmatrix} c_{11}l_x^2 + c_{66}l_y^2 + c_{44}l_z^2 + 2c_{16}l_xl_y & c_{16}(l_x^2 - l_y^2) + (c_{12}+c_{66})l_xl_y & (c_{13}+c_{44})l_zl_x \\ c_{16}(l_x^2 - l_y^2) + (c_{12}+c_{66})l_xl_y & c_{66}l_x^2 + c_{11}l_y^2 + c_{44}l_z^2 - 2c_{16}l_xl_y & (c_{13}+c_{44})l_yl_z \\ (c_{13}+c_{44})l_zl_x & (c_{13}+c_{44})l_yl_z & c_{44}(l_x^2 + l_y^2) + c_{33}l_z^2 \end{bmatrix}$$

$$\times \begin{bmatrix} v_x \\ v_y \\ v_z \end{bmatrix} = \rho\omega^2\begin{bmatrix} v_x \\ v_y \\ v_z \end{bmatrix}.$$

ORTHORHOMBIC

$$k^2\begin{bmatrix} c_{11}l_x^2 + c_{66}l_y^2 + c_{55}l_z^2 & (c_{12}+c_{66})l_xl_y & (c_{13}+c_{55})l_zl_x \\ (c_{12}+c_{66})l_xl_y & c_{66}l_x^2 + c_{22}l_y^2 + c_{44}l_z^2 & (c_{23}+c_{44})l_yl_z \\ (c_{13}+c_{55})l_zl_x & (c_{23}+c_{44})l_yl_z & c_{55}l_x^2 + c_{44}l_y^2 + c_{33}l_z^2 \end{bmatrix}\begin{bmatrix} v_x \\ v_y \\ v_z \end{bmatrix} = \rho\omega^2\begin{bmatrix} v_x \\ v_y \\ v_z \end{bmatrix}$$

B. SLOWNESS SURFACES FOR ISOTROPIC AND ANISOTROPIC SOLIDS

This section gives slowness curves for the principal planes of all crystal classes except triclinic and monoclinic. Representative dimensions on these curves are stated in terms of the material parameters, neglecting the piezoelectric effect. Using the material constants given in Appendix 2, these dimensions can be easily evaluated for any material and then used to sketch the general shape of the curves.

B.1 Isotropic

In Section C of Chapter 6 it was seen that the phase velocity $V_p = \omega/k$ is independent of direction and has two values,

$$V_l = \sqrt{\frac{c_{11}}{\rho}} = \sqrt{\frac{\lambda + 2\mu}{\rho}}$$

for the longitudinal wave, and

$$V_s = \sqrt{\frac{c_{44}}{\rho}} = \sqrt{\frac{\mu}{\rho}}$$

for the two shear waves. The slowness surface consists of two concentric spheres (Fig. 3.1). Since the Lamé constants λ and μ are both positive, the outer sphere is for shear waves and the inner one for longitudinal waves.

B.2 Cubic

The case of a cubic material was treated in Examples 4 and 5 of Chapter 7. For propagation in a cube face the characteristic equation factors into a linear term and a quadratic term. There is a pure shear wave polarized normal to the cube face,

$$\left(\frac{k}{\omega}\right)_1 = \left(\frac{\rho}{c_{44}}\right)^{1/2}, \tag{3.1}$$

a quasishear wave,

$$\left(\frac{k}{\omega}\right)_2 = (2\rho)^{1/2}\left\{c_{11} + c_{44} - \sqrt{(c_{11} - c_{44})^2\cos^2 2\phi + (c_{12} + c_{44})^2\sin^2 2\phi}\right\}^{-1/2} \tag{3.2}$$

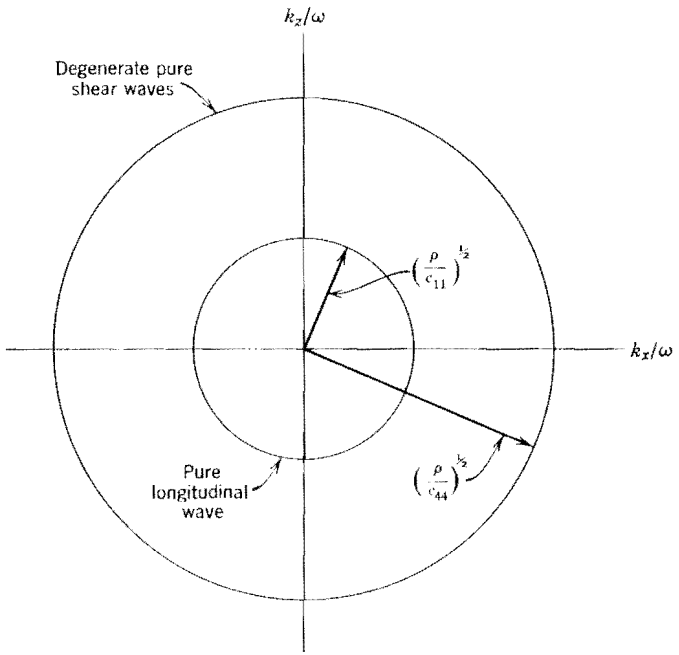

FIGURE 3.1. **Isotropic. Propagation in an arbitrary plane.**

and a quasilongitudinal wave,

$$\left(\frac{k}{\omega}\right)_3 = (2\rho)^{1/2}\left\{c_{11} + c_{44} + \sqrt{(c_{11} - c_{44})^2 \cos^2 2\phi + (c_{12} + c_{44})^2 \sin^2 2\phi}\right\}^{-1/2}, \tag{3.3}$$

where $\cos\phi = l_x$. Inverse velocity curves are shown in Fig. 3.2 for gallium arsenide. Representative dimensions are given in terms of material parameters. From these, the general shape of the curves can be deduced for any cubic material.

For propagation in a plane passing through a cube face diagonal the characteristic equation again factors into linear and quadratic terms. There is a pure shear mode polarized normal to the plane of propagation,

$$\left(\frac{k}{\omega}\right)_2 = \left(\frac{\rho}{\frac{c_{11} - c_{12}}{2}\cos^2\theta + c_{44}\sin^2\theta}\right)^{1/2}, \tag{3.4}$$

a quasishear wave,

$$\left(\frac{k}{\omega}\right)_1 = \left(\frac{2\rho}{B - \sqrt{B^2 - C}}\right)^{1/2}, \tag{3.5}$$

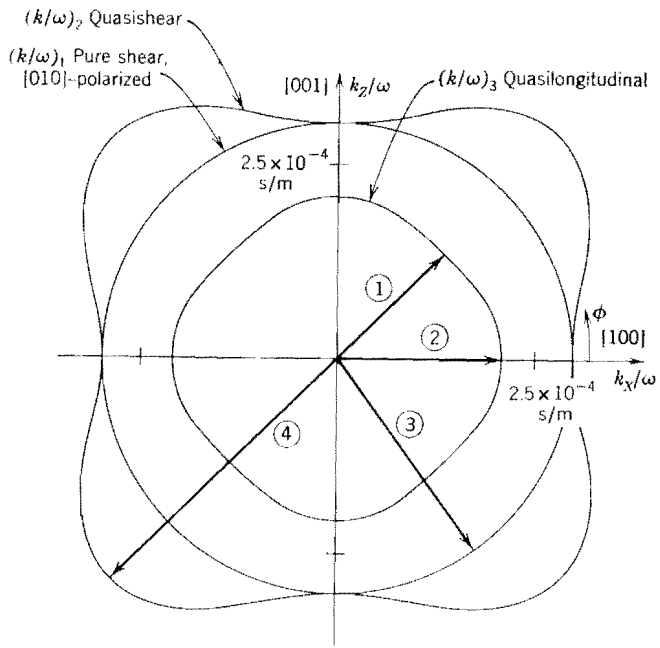

(1) $\left(\frac{\rho}{c_{11} + c_{44}(1 - 1/A)}\right)^{1/2}$ (3) $(\rho/c_{44})^{1/2}$

(2) $(\rho/c_{11})^{1/2}$ (4) $(\rho A/c_{44})^{1/2}$

Anisotropy factor $A = \dfrac{2c_{44}}{c_{11} - c_{12}}$

FIGURE 3.2. **Cubic crystal classes. Propagation in a cube face. Curves shown are for GaAs, with the piezoelectric effect ignored. Sketches may be made for other materials, using the key dimensions shown.**

and a quasilongitudinal wave,

$$\left(\frac{k}{\omega}\right)_3 = \left(\frac{2\rho}{B + \sqrt{B^2 - C}}\right)^{1/2} \tag{3.6}$$

Here

$$B = (c_{11} + c_{12} + 4c_{44})\frac{\cos^2\theta}{2} + (c_{11} + c_{44})\sin^2\theta$$

and

$$C = (c_{11}c'_{11} - c_{12}^2 - 2c_{12}c_{44})\sin^2 2\theta + 4c_{44}(c'_{11}\cos^4\theta + c_{11}\sin^4\theta)$$

with

$$c'_{11} = \frac{c_{11} + c_{12} + 2c_{44}}{2}.$$

The direction angle θ is defined in Fig. 3.3, which gives curves for gallium arsenide and also some representative dimensions.

B.3 Hexagonal

For hexagonal materials the characteristic equation factors when propagation is in the XY plane, that is, normal to the Z-axis. The dispersion relation is

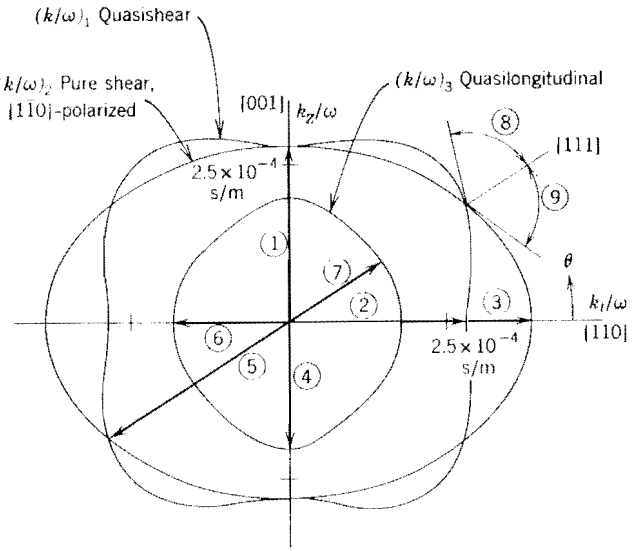

(1)(2) $(\rho/c_{44})^{1/2}$

(3) $(\rho A/c_{44})^{1/2}$

(4) $(\rho/c_{11})^{1/2}$

(5) $\left(\dfrac{3\rho A}{(2+A)c_{44}}\right)^{1/2}$

(6) $\left(\dfrac{\rho}{c_{11} + c_{44}\left(\dfrac{A-1}{A}\right)}\right)^{1/2}$

(7) $\left(\dfrac{3\rho}{3c_{11} + 4c_{44}\left(\dfrac{A-1}{A}\right)}\right)^{1/2}$

(8)(9) $\cot^{-1}\sqrt{2}\left(\dfrac{A-1}{A+2}\right)$

Anisotropy factor

$$A = \frac{2c_{44}}{c_{11} - c_{12}}$$

FIGURE 3.3. **Cubic crystal classes. Propagation in a cube diagonal plane. Curves shown are for GaAs, with the piezoelectric effect ignored.**

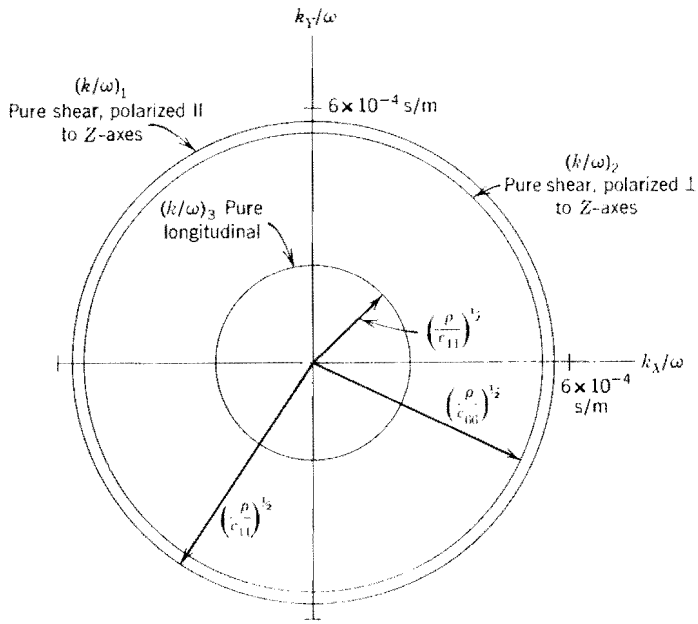

FIGURE 3.4. **Hexagonal crystal classes. Propagation normal to the Z-axis. Curves are for CdS, with the piezoelectric effect ignored.**

independent of the propagation direction in this plane. There is one pure shear mode

$$\left(\frac{k}{\omega}\right)_2 = \left(\frac{\rho}{c_{66}}\right)^{1/2}, \tag{3.7}$$

polarized normal to the Z axis, another pure shear mode

$$\left(\frac{k}{\omega}\right)_t = \left(\frac{\rho}{c_{44}}\right)^{1/2} \tag{3.8}$$

polarized parallel to the Z axis, and a pure longitudinal mode

$$\left(\frac{k}{\omega}\right)_3 = \left(\frac{\rho}{c_{11}}\right)^{1/2}. \tag{3.9}$$

Figure 3.4 shows curves for cadmium sulfide, neglecting the piezoelectric effect.

The characteristic equation also factors for propagation in the XZ plane. Since the Christoffel equation can be shown to be symmetric with respect to an arbitrary rotation about the Z-axis the same dispersion relation will apply

for any meridian plane. That is, the wave vector surface is always rotationally symmetric. There is one pure shear mode

$$\left(\frac{k}{\omega}\right)_2 = \left(\frac{\rho}{c_{66}\sin^2\theta + c_{44}\cos^2\theta}\right)^{1/2}, \tag{3.10}$$

polarized normal to the meridian plane containing **k**. The other solutions are a quasishear wave

$$\left(\frac{k}{\omega}\right)_1 = (2\rho)^{1/2}\Big\{c_{11}\sin^2\theta + c_{33}\cos^2\theta + c_{44} - \sqrt{[(c_{11}-c_{44})\sin^2\theta + (c_{44}-c_{33})\cos^2\theta]^2 + (c_{13}+c_{44})^2\sin^2 2\theta}\Big\}^{-1/2}. \tag{3.11}$$

and a quasilongitudinal wave

$$\left(\frac{k}{\omega}\right)_3 = (2\rho)^{1/2}\Big\{c_{11}\sin^2\theta + c_{33}\cos^2\theta + c_{44} + \sqrt{[(c_{11}-c_{44})\sin^2\theta + (c_{44}-c_{33})\cos^2\theta]^2 + (c_{13}+c_{44})^2\sin^2 2\theta}\Big\}^{-1/2}. \tag{3.12}$$

The direction angle θ is measured from the Z axis (Fig. 3.5).

B.4 Trigonal

B.4a Classes *32*, *3m*, $\bar{3}m$. In this case, the characteristic equation factors only for propagation in the YZ plane or for propagation along the X, Y, and Z axes.

For X propagation there are two pure shear waves

$$\left(\frac{k}{\omega}\right)_1 = (2\rho)^{1/2}\Big\{c_{44} + c_{66} + \sqrt{(c_{66}-c_{44})^2 + 4c_{14}^2}\Big\}^{-1/2} \tag{3.13}$$

$$\left(\frac{k}{\omega}\right)_2 = (2\rho)^{1/2}\Big\{c_{44} + c_{66} - \sqrt{(c_{66}-c_{44})^2 + 4c_{14}^2}\Big\}^{-1/2} \tag{3.14}$$

and a pure longitudinal wave

$$\left(\frac{k}{\omega}\right)_3 = \left(\frac{\rho}{c_{11}}\right)^{1/2}. \tag{3.15}$$

Along Y there is one pure shear wave

$$\left(\frac{k}{\omega}\right)_2 = \left(\frac{\rho}{c_{66}}\right)^{1/2} \tag{3.16}$$

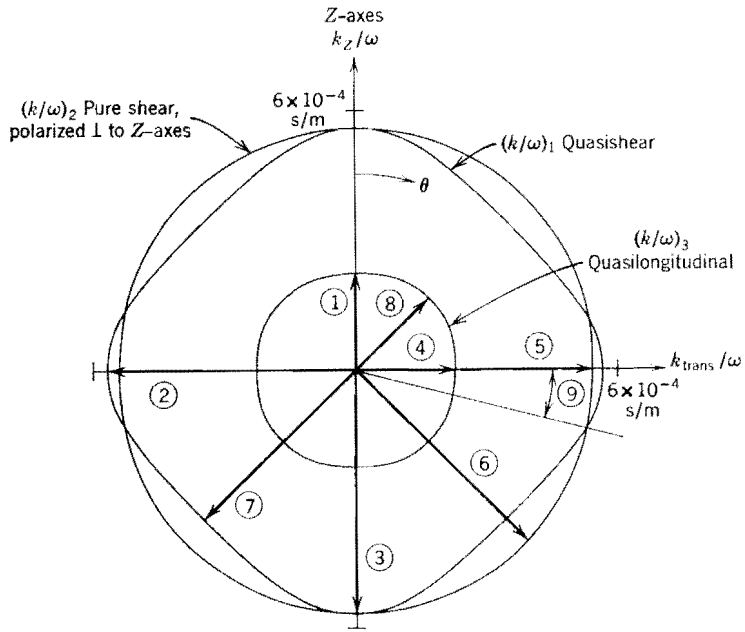

(1) $(\rho/c_{33})^{1/2}$

(2) $(\rho/c_{44})^{1/2}$

(3) $(\rho/c_{44})^{1/2}$

(4) $(\rho/c_{11})^{1/2}$

(5) $(\rho/c_{66})^{1/2}$

(6) $\left(\dfrac{2\rho}{c_{66}+c_{44}}\right)^{1/2}$

(7) $\dfrac{(4\rho)^{1/2}}{\{c_{11}+c_{33}+2c_{44}-\sqrt{(c_{11}-c_{33})^2+4(c_{13}+c_{44})^2}\}^{1/2}}$

(8) $\dfrac{(4\rho)^{1/2}}{\{c_{11}+c_{33}+2c_{44}+\sqrt{(c_{11}-c_{33})^2+4(c_{13}+c_{44})^2}\}^{1/2}}$

(9) $\cot^{-1}\sqrt{\dfrac{(c_{13}+c_{44})^2-(c_{11}-c_{66})(c_{33}-c_{44})}{(c_{44}-c_{66})(c_{11}-c_{66})}}$

FIGURE 3.5. Hexagonal crystal classes. Propagation in a meridian plane. Curves shown are for CdS, with the piezoelectric effect ignored.

polarized along X. The quasishear wave is

$$\left(\frac{k}{\omega}\right)_1 = (2\rho)^{1/2}\Big\{(c_{44}+c_{11}) - \sqrt{(c_{11}-c_{44})^2 + 4c_{14}^2}\Big\}^{-1/2} \tag{3.17}$$

and the quasilongitudinal wave is

$$\left(\frac{k}{\omega}\right)_3 = (2\rho)^{1/2}\Big\{(c_{44}+c_{11}) + \sqrt{(c_{11}-c_{44})^2 + 4c_{14}^2}\Big\}^{-1/2} \tag{3.18}$$

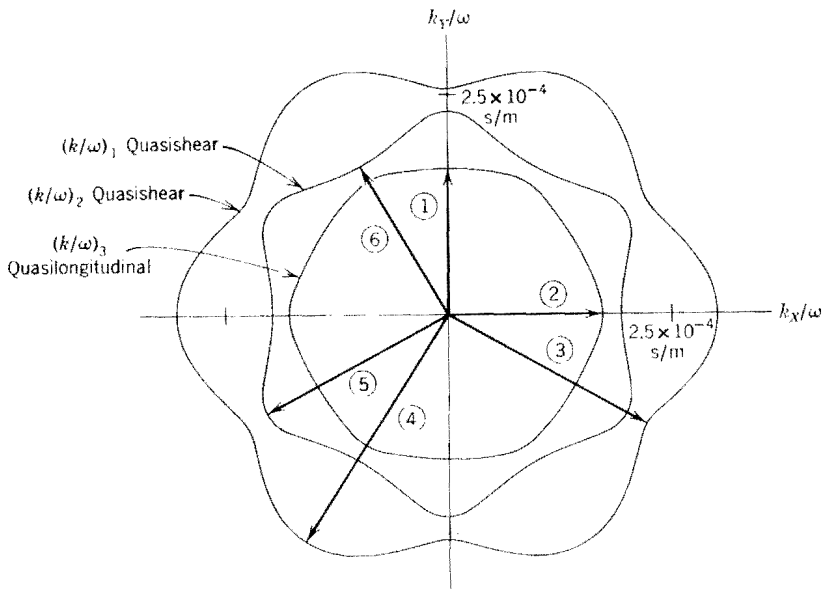

(1) $\left(\dfrac{2\rho}{c_{11}+c_{44}+c'}\right)^{1/2}$

(2) $(\rho/c_{11})^{1/2}$

(3) $(\rho/c_{66})^{1/2}$

(4) $\left(\dfrac{2\rho}{c_{44}+c_{66}-c''}\right)^{1/2}$

(5) $\left(\dfrac{2\rho}{c_{11}+c_{44}-c'}\right)^{1/2}$

(6) $\left(\dfrac{2\rho}{c_{44}+c_{66}+c''}\right)^{1/2}$

$c' = \{(c_{11}-c_{44})^2+4c_{14}^2\}^{1/2}$

$c'' = \{(c_{66}-c_{44})^2+4c_{14}^2\}^{1/2}$

FIGURE 3.6. **Trigonal crystal classes *32*, *3m*, $\bar{3}m$. Propagation normal to the *Z*-axis. Curves shown are for quartz, with the piezoelectric effect ignored.**

Because of the threefold symmetry about the *Z*-axis and the inherent inversion symmetry of the elastic stiffness matrix the wave vector curves have a sixfold pattern in the *XY* plane (Fig. 3.6). Piezoelectric stiffening (Part 4 of Section 8.F) is usually only a small correction to the dispersion curves and has been neglected in calculating the curves shown for quartz.

In the *YZ* plane a pure shear wave, with polarization along the *X* axis, is governed by the relation

$$\left(\frac{k}{\omega}\right)_2 = \rho^{1/2}\{c_{66}\sin^2\theta + c_{44}\cos^2\theta + c_{14}\sin 2\theta\}^{-1/2} \tag{3.19}$$

The quasishear wave is described by

$$\left(\frac{k}{\omega}\right)_1 = (2\rho)^{1/2}\{A - \sqrt{B^2+C}\}^{-1/2} \tag{3.20}$$

and the quasilongitudinal wave by

$$\left(\frac{k}{\omega}\right)_3 = (2\rho)^{1/2}\{A + \sqrt{B^2+C}\}^{-1/2}, \tag{3.21}$$

where

$$A = c_{44} + c_{11}\sin^2\theta + c_{33}\cos^2\theta - c_{14}\sin 2\theta$$
$$B = (c_{44}-c_{11})\sin^2\theta + (c_{33}-c_{44})\cos^2\theta + c_{14}\sin 2\theta$$
$$C = ((c_{13}+c_{44})\sin 2\theta - 2c_{14}\sin^2\theta)^2.$$

Figure 3.7 shows curves for quartz. The characteristic equation does not factor for propagation in the *XZ* plane and little information can be obtained without numerical computation. For propagation along *Z* the pure shear waves are degenerate,

$$\left(\frac{k}{\omega}\right)_1 = \left(\frac{k}{\omega}\right)_2 = \left(\frac{\rho}{c_{44}}\right)^{1/2}, \tag{3.22}$$

and the pure longitudinal wave is governed by

$$\left(\frac{k}{\omega}\right)_3 = \left(\frac{\rho}{c_{33}}\right)^{1/2}. \tag{3.23}$$

Along *X* there are pure shear waves (3.13) and (3.14), and a pure longitudinal wave (3.15). Curves for quartz are given in Fig. 3.8.

B.4b Classes *3*, $\bar{3}$. In this case it is possible to deduce the general shape of the slowness curves for these crystal classes by noting that the stiffness matrix (given in Part A.5 of Appendix 2) assumes exactly the same form as for classes *32*, *3m*, $\bar{3}m$ when it is referred to a set of coordinate axes that are rotated clockwise through an angle ξ, with

$$\tan 3\xi = \frac{c_{25}}{c_{14}}, \tag{3.24}$$

about the *Z* axis. The general shape of the slowness curves for classes *3* and $\bar{3}$, referred to the crystal axis directions, is thus obtained by rotating the curves in Fig. 3.6 to 3.8 *counterclockwise* through the angle ξ about the *Z* axis.† Because there are no measured stiffness constants for materials of this kind,

† It should be noted, however, that the dimensions given in these figures cannot be calculated *directly* from the stiffness constants referred to the crystal axes. The *transformed* stiffness constants must be evaluated first.

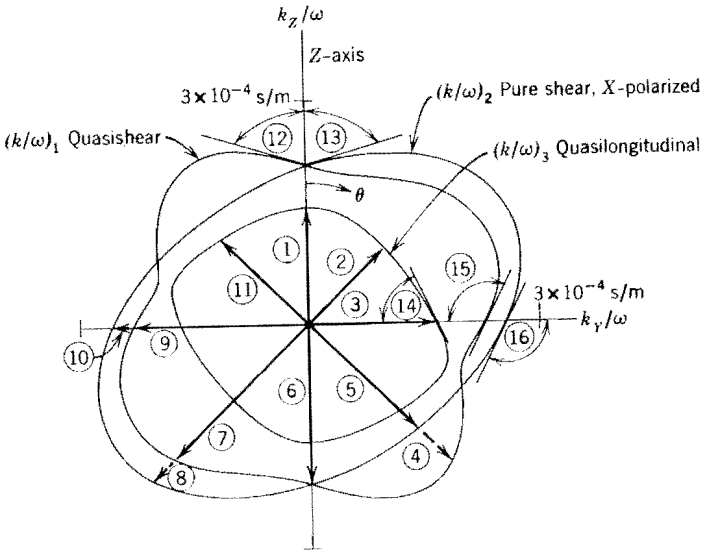

(1) $(\rho/c_{33})^{1/2}$

(2) $\left(\dfrac{4\rho}{c_{11}+c_{33}+2(c_{44}-c_{14})+c'''}\right)^{1/2}$

(3) $\dfrac{(2\rho)^{1/2}}{(c_{11}+c_{44}+c')^{1/2}}$

(4) $\left(\dfrac{4\rho}{c_{11}+c_{33}+2(c_{44}+c_{14})-c''''}\right)^{1/2}$

(5) $\dfrac{(2\rho)^{1/2}}{(c_{44}+c_{66}-2c_{14})^{1/2}}$

(6) $(\rho/c_{44})^{1/2}$

(7) $\left(\dfrac{4\rho}{c_{11}+c_{33}+2(c_{44}-c_{14})-c'''}\right)^{1/2}$

(8) $\dfrac{(2\rho)^{1/2}}{(c_{44}+c_{66}+2c_{14})^{1/2}}$

(9) $\dfrac{(2\rho)^{1/2}}{(c_{11}+c_{44}-c')^{1/2}}$

(10) $(\rho/c_{66})^{1/2}$

(11) $\left(\dfrac{4\rho}{c_{11}+c_{33}+2(c_{44}+c_{14})+c''''}\right)^{1/2}$

(12) (13) $\cot^{-1} c_{14}/c_{44}$

(14) $\cot^{-1}\dfrac{-c_{14}(c_{11}+c_{44}+2c_{13}+c')}{c'(c_{11}+c_{44}+c')}$

(15) $\cot^{-1}\dfrac{c_{14}(c_{11}+c_{44}+2c_{13}-c')}{c'(c_{11}+c_{44}-c')}$

(16) $\cot^{-1} c_{14}/c_{66}$

$c' = \{(c_{11}-c_{44})^2+4c_{14}^2\}^{1/2}$

$c''' \quad c'''' = \{(c_{33}-c_{11}\pm 2c_{14})^2+4(c_{44}+c_{13}\mp c_{14})^2\}^{1/2}$

FIGURE 3.7. **Trigonal crystal classes *32*, *3m*, $\bar{3}m$. Propagation in the *YZ* plane. Curves shown are for quartz, with the piezoelectric effect ignored.**

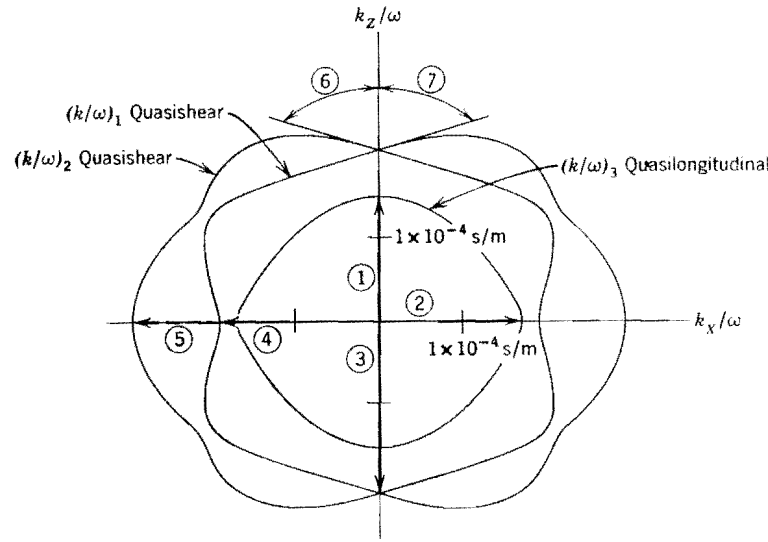

(1) $(\rho/c_{33})^{1/2}$

(2) $(\rho/c_{11})^{1/2}$

(3) $(\rho/c_{44})^{1/2}$

(4) $\left(\dfrac{2\rho}{c_{44}+c_{66}+c''}\right)^{1/2}$

(5) $\left(\dfrac{2\rho}{c_{44}+c_{66}-c''}\right)^{1/2}$

(6)(7) $\cot^{-1} -c_{14}/c_{44}$

$c'' = \{(c_{66}-c_{44})^2+4c_{14}^2\}^{1/2}$

FIGURE 3.8. **Trigonal crystal classes *32*, *3m*, $\bar{3}m$. Propagation in the *XZ* plane. Curves shown are for quartz, with the piezoelectric effect ignored.**

sample curves cannot be given. However, the same phenomenon occurs in the tetragonal classes and will be illustrated below.

B.5 Tetragonal

B.5a Classes *4mm*, *422*, $\bar{4}2m$, *4/mmm*. The characteristic equation factors for propagation in the *XY* and *XZ* (or *YZ*) planes.

In the *XY* plane

$$\left(\frac{k}{\omega}\right)_1 = \left(\frac{\rho}{c_{44}}\right)^{1/2} \tag{3.25}$$

is a pure shear wave polarized along *Z*. The quasishear wave is

$$\left(\frac{k}{\omega}\right)_2 = (2\rho)^{1/2}\{c_{11}+c_{66}-\sqrt{(c_{11}-c_{66})^2\cos^2 2\phi+(c_{12}+c_{66})^2\sin^2 2\phi}\}^{-1/2} \tag{3.26}$$

and the quasilongitudinal wave is

$$\left(\frac{k}{\omega}\right)_3 = (2\rho)^{1/2}\left\{c_{11} + c_{66} + \sqrt{(c_{11} - c_{66})^2 \cos^2 2\phi + (c_{12} + c_{66})^2 \sin^2 2\phi}\right\}^{-1/2}, \tag{3.27}$$

where the angle ϕ is defined in Fig. 3.9. These expressions are the same as for hexagonal crystals, except that there is now no restriction on c_{66}. The consequences of this are (1) the slowness surfaces are no longer rotationally symmetric and (2) there is only one pure mode propagating in the XY plane.

In the XZ plane there is a pure shear wave polarized along Y,

$$\left(\frac{k}{\omega}\right)_2 = \rho^{1/2}\{c_{66}\sin^2\theta + c_{44}\cos^2\theta\}^{-1/2}. \tag{3.28}$$

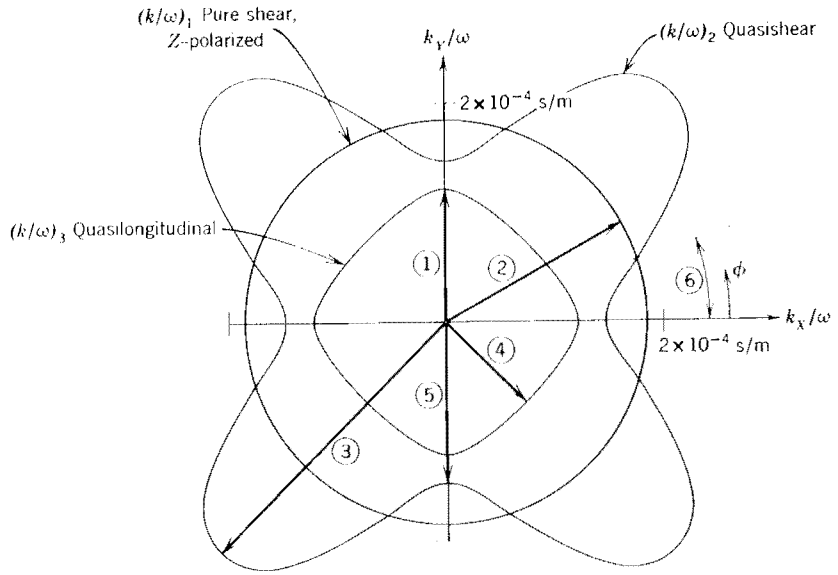

(1) $(\rho/c_{11})^{1/2}$

(2) $(\rho/c_{44})^{1/2}$

(3) $\left(\dfrac{2\rho}{c_{11} - c_{12}}\right)^{1/2}$

(4) $\left(\dfrac{2\rho}{c_{11} + 2c_{66} + c_{12}}\right)^{1/2}$

(5) $(\rho/c_{66})^{1/2}$

(6) $\sin^2\phi = \frac{1}{2} \pm \sqrt{\frac{1}{4} + F}$

$$F = \frac{(c_{11} - c_{44})(c_{66} - c_{44})}{(c_{11} - c_{66})^2 - (c_{12} + c_{66})^2}$$

FIGURE 3.9. **Tetragonal crystal classes** *4mm*, *422*, $\bar{4}2m$, *4/mmm*. **Propagation in the** XY **plane. Curves shown are for rutile.**

The quasishear wave is described by

$$\left(\frac{k}{\omega}\right)_1 = (2\rho)^{1/2}\left\{A - \sqrt{B^2 + C}\right\}^{-1/2} \tag{3.29}$$

and the quasilongitudinal wave by

$$\left(\frac{k}{\omega}\right)_3 = (2\rho)^{1/2}\left\{A + \sqrt{B^2 + C}\right\}^{-1/2}, \tag{3.30}$$

where

$$A = c_{11}\sin^2\theta + c_{33}\cos^2\theta + c_{44}$$
$$B = (c_{11} - c_{44})\sin^2\theta + (c_{44} - c_{33})\cos^2\theta$$
$$C = (c_{13} + c_{44})^2 \sin^2 2\theta$$

Curves for rutile are shown in Fig. 3.10.

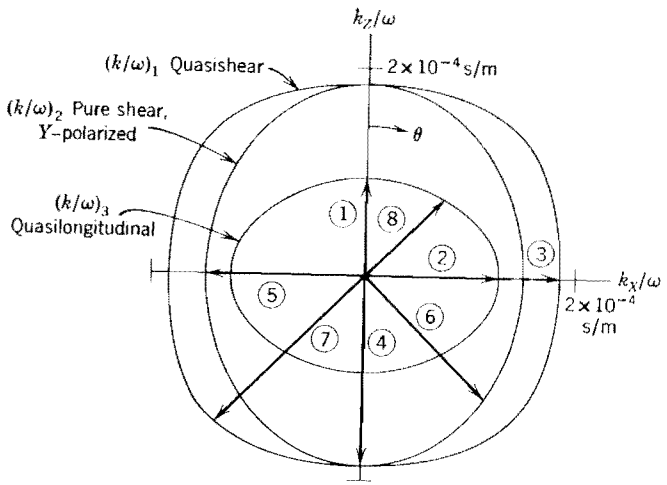

(1) $(\rho/c_{33})^{1/2}$

(2) $(\rho/c_{11})^{1/2}$

(3)(4) $(\rho/c_{44})^{1/2}$

(5) $(\rho/c_{66})^{1/2}$

(6) $\left(\dfrac{2\rho}{c_{66} + c_{44}}\right)^{1/2}$

(7) $$\frac{(4\rho)^{1/2}}{\left\{c_{11} + c_{33} + 2c_{44} - \sqrt{(c_{11} - c_{33})^2 + 4(c_{13} + c_{44})^2}\right\}^{1/2}}$$

(8) $$\frac{(4\rho)^{1/2}}{\left\{c_{11} + c_{33} + 2c_{44} + \sqrt{(c_{11} - c_{33})^2 + 4(c_{13} + c_{44})^2}\right\}^{1/2}}$$

FIGURE 3.10. **Tetragonal crystal classes** *4mm*, *422*, $\bar{4}2m$, *4/mmm*. **Propagation in the** XZ **plane. Curves shown are for rutile.**

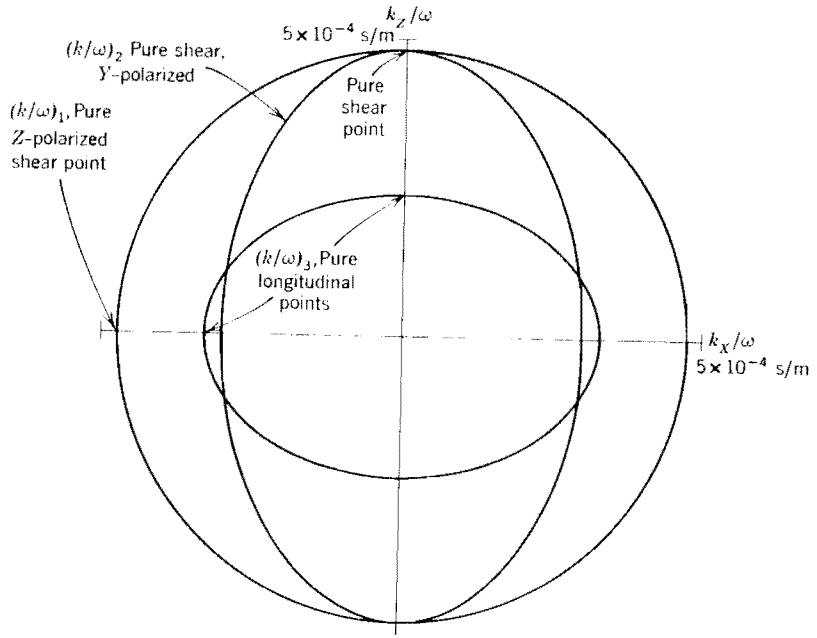

FIGURE 3.11. **Slowness curves for tellurium dioxide, corresponding to Fig. 3.10.**

One material of this crystal class (tellurium dioxide) has the interesting property that $c_{66} > c_{11}$, while c_{44} satisfies the usual condition $c_{44} < c_{11}$. This means that the X-intercept (5) in Fig. 3.10 falls *inside* the X-intercept (2). From this it appears that the $(k/\omega)_2$ and $(k/\omega)_3$ curves should cross each other. Figure 3.11 shows that this does occur. Along the X axis, the longitudinal wave has the unusual property of being slower than one of the shear waves; but normal conditions are restored after the curves have crossed. Figure 3.12 shows slowness curves in the XY plane for the same material. In this case, the solution $(k/\omega)_3$ changes from pure longitudinal to pure shear as ϕ increases from 0° to 45°, and the solution $(k/\omega)_2$ changes from pure shear to pure longitudinal.

B.5b Classes 4, $\bar{4}$, $4/m$. The characteristic equation factors only for propagation in the XY plane and along the Z axis.

In the XY plane there is a pure shear wave polarized along Z,

$$\left(\frac{k}{\omega}\right)_1 = \left(\frac{\rho}{c_{11}}\right)^{1/2}. \tag{3.31}$$

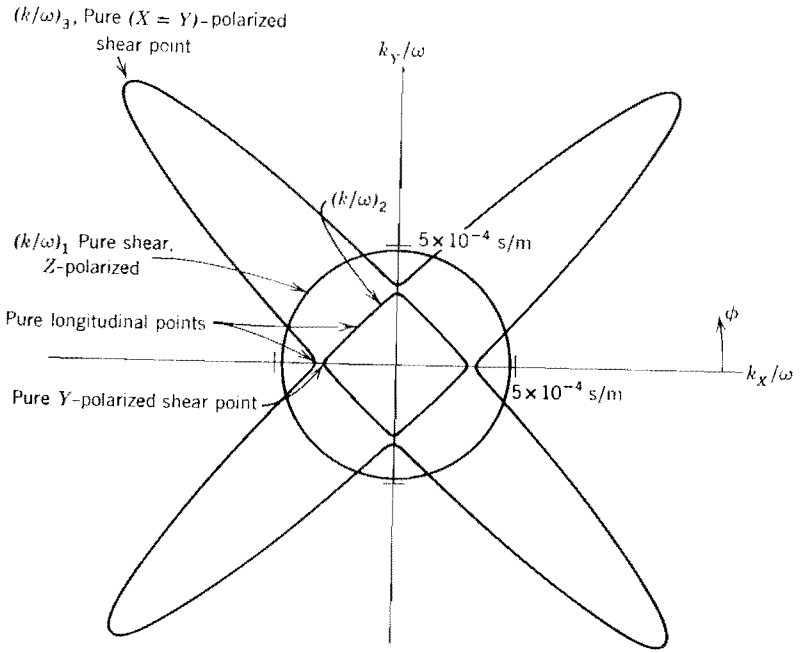

FIGURE 3.12. **Slowness curves for tellurium dioxide, corresponding to Fig. 3.9.**

For the quasishear wave

$$\left(\frac{k}{\omega}\right)_2 = (2\rho)^{1/2}\left\{c_{11} + c_{66} - \sqrt{(c_{11} + c_{66})^2 - 4C}\right\}^{-1/2} \tag{3.32}$$

and for the quasilongitudinal wave

$$\left(\frac{k}{\omega}\right)_3 = (2\rho)^{1/2}\left\{c_{11} + c_{66} + \sqrt{(c_{11} + c_{66})^2 - 4C}\right\}^{-1/2}. \tag{3.33}$$

where

$$C = (c_{11}\cos^2\phi + c_{66}\sin^2\phi + c_{16}\sin 2\phi)(c_{11}\sin^2\phi + c_{66}\cos^2\phi - c_{16}\sin 2\phi) - (c_{16}\cos 2\phi + (c_{12} + c_{66})\sin\phi\cos\phi)^2.$$

Along the Z axis there are two degenerate shear waves

$$\left(\frac{k}{\omega}\right)_1 = \left(\frac{k}{\omega}\right)_2 = \left(\frac{\rho}{c_{44}}\right)^{1/2}$$

and a pure longitudinal wave.

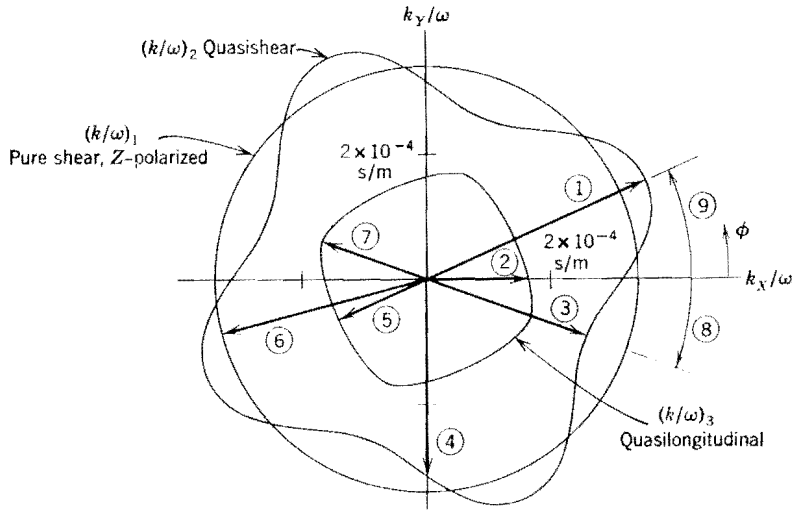

(1) $\left(\dfrac{2\rho}{c'_{11}-c'_{12}}\right)^{1/2}$

(2) $(2\rho)^{1/2}\left\{c_{11}+c_{66}+\sqrt{(c_{11}-c_{66})^2+4c_{16}^2}\right\}^{1/2}$

(3) $\left(\dfrac{\rho}{c'_{66}}\right)^{1/2}$

(4) $(2\rho)^{1/2}\left\{c_{11}+c_{66}-\sqrt{(c_{11}-c_{66})^2+4c_{16}^2}\right\}^{1/2}$

(5) $\left(\dfrac{2\rho}{c'_{11}+2c'_{66}+c'_{12}}\right)^{1/2}$

(6) $\left(\dfrac{\rho}{c_{44}}\right)^{1/2}$

(7) $\left(\dfrac{\rho}{c'_{11}}\right)^{1/2}$

(8) $\tan 4\phi_{ma}=\dfrac{-4c_{16}}{c_{11}-c_{12}-2c_{16}}$

(9) $\phi_{mi}=\dfrac{\pi}{4}-\phi_{ma}$

$$c'_{11}=c_{11}(\cos^4\phi_{ma}+\sin^4\phi_{ma})+\tfrac{1}{2}c_{12}\sin^2 2\phi_{ma}-c_{16}\sin 4\phi_{ma}+c_{66}\sin^2 2\phi_{ma}$$

$$c'_{12}=\tfrac{1}{2}c_{11}\sin^2 2\phi_{ma}+c_{12}(\cos^4\phi_{ma}+\sin^4\phi_{ma})+c_{16}\sin 4\phi_{ma}-c_{66}\sin^2 2\phi_{ma}$$

$$c'_{66}=(c_{11}-c_{12})\sin^2 2\phi_{ma}+c_{16}\sin 4\phi_{ma}+c_{66}\cos^2 2\phi_{ma}$$

FIGURE 3.13. **Tetragonal classes *4*, $\bar{4}$, *4/m*. Propagation in the *XY* plane. Curves are for calcium molybdate.**

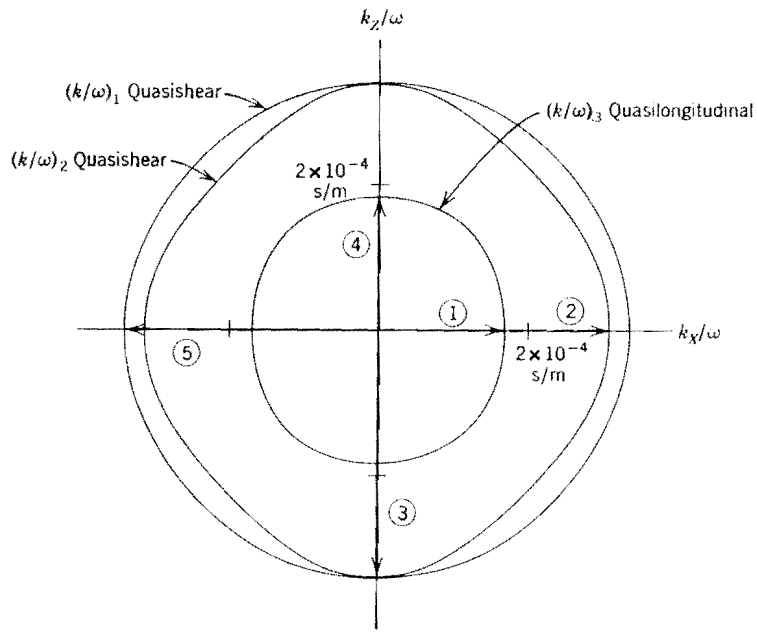

(1) $(2\rho)^{1/2}\left\{c_{11}+c_{66}+\sqrt{(c_{11}-c_{66})^2+4c_{16}^2}\right\}^{1/2}$

(2) $(2\rho)^{1/2}\left\{c_{11}+c_{66}-\sqrt{(c_{11}-c_{66})^2+4c_{16}^2}\right\}^{1/2}$

(3) $(\rho/c_{44})^{1/2}$

(4) $(\rho/c_{33})^{1/2}$

(5) $(\rho/c_{44})^{1/2}$

FIGURE 3.14. **Tetragonal classes *4*, $\bar{4}$, *4/m*. Propagation in the *XZ* plane. Curves are for calcium molybdate.**

The stiffness matrix for materials of this kind can be converted to the same form as for classes *4mm*, *422*, $\bar{4}$*2m*, *4/mmm* by performing an appropriate rotation of coordinates about the *Z* axis. Slowness curves therefore have the same general appearance as Fig. 3.9, but are rotated about the *Z* axis. Curves for calcium molybdate are shown in Figs. 3.13 to 3.15.

B.6 Orthorhombic

The characteristic equation is of the same form as for the hexagonal classes, but with more general stiffness coefficients. It factors for propagation in the *XY*, *XZ*, and *YZ* planes.

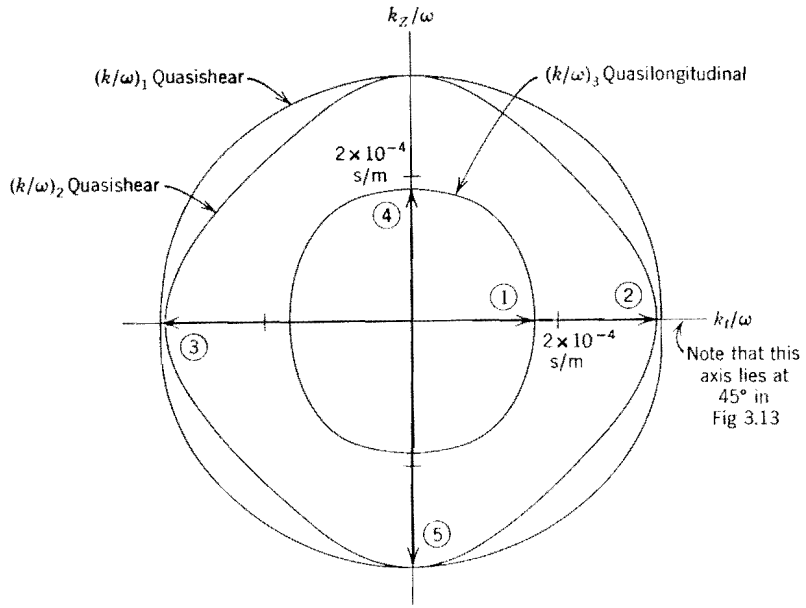

(1) $\left(\dfrac{2\rho}{c_{11}+c_{66}+\sqrt{(c_{12}+c_{66})^2+4c_{16}^2}}\right)^{1/2}$

(2) $\left(\dfrac{2\rho}{c_{11}+c_{66}-\sqrt{(c_{12}+c_{66})^2+4c_{16}^2}}\right)^{1/2}$

(3) $(\rho/c_{44})^{1/2}$

(4) $(\rho/c_{33})^{1/2}$

(5) $(\rho/c_{44})^{1/2}$

FIGURE 3.15. **Tetragonal classes 4, $\bar{4}$, 4/m. Propagation in the plane $X = Y, Z$. Curves are for calcium molybdate.**

In the XY plane there is a pure shear wave polarized along the Z axis,

$$\left(\frac{k}{\omega}\right)_1 = \rho^{1/2}\{c_{44}\cos^2\phi + c_{55}\sin^2\phi\}^{-1/2}. \tag{3.34}$$

The quasishear wave is

$$\left(\frac{k}{\omega}\right)_2 = (2\rho)^{1/2}\Big\{c_{66} + c_{11}\cos^2\phi + c_{22}\sin^2\phi - \sqrt{(c_{66} + c_{11}\cos^2\phi + c_{22}\sin^2\phi)^2 - 4C}\Big\}^{-1/2} \tag{3.35}$$

and the quasilongitudinal wave is

$$\left(\frac{k}{\omega}\right)_3 = (2\rho)^{1/2}\Big\{c_{66} + c_{11}\cos^2\phi + c_{22}\sin^2\phi + \sqrt{(c_{66} + c_{11}\cos^2\phi + c_{22}\sin^2\phi)^2 - 4C}\Big\}^{-1/2} \tag{3.36}$$

where

$$C = (c_{11}\cos^2\phi + c_{66}\sin^2\phi)(c_{66}\cos^2\phi + c_{22}\sin^2\phi) - (c_{12} + c_{66})^2\cos^2\phi\sin^2\phi.$$

The direction angle ϕ is defined in Fig. 3.16, which shows curves for barium sodium niobate, neglecting the piezoelectric effect.

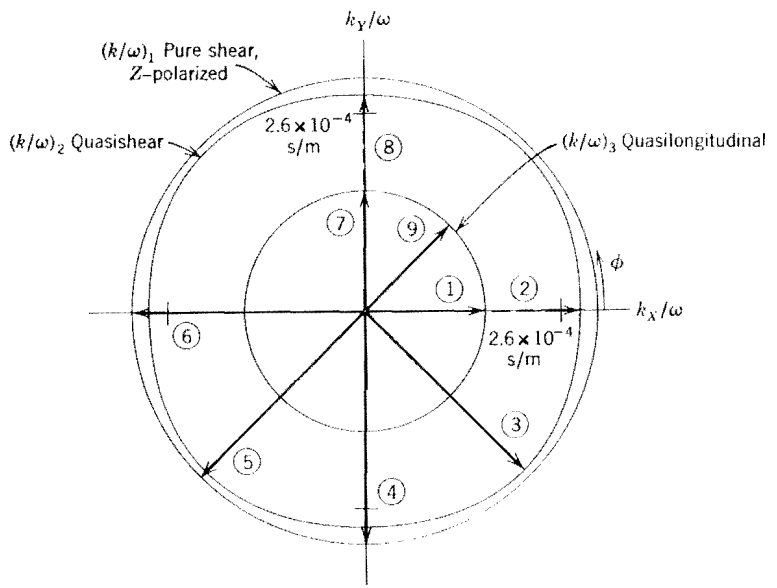

(1) $(\rho/c_{11})^{1/2}$

(2) $(\rho/c_{66})^{1/2}$

(3) $\left(\dfrac{4\rho}{c_{11}+c_{22}+2c_{66}-\sqrt{(c_{11}-c_{22})^2+4(c_{12}+c_{66})^2}}\right)^{1/2}$

(4) $(\rho/c_{44})^{1/2}$

(5) $\left(\dfrac{2\rho}{c_{44}+c_{55}}\right)^{1/2}$

(6) $(\rho/c_{55})^{1/2}$

(7) $(\rho/c_{22})^{1/2}$

(8) $(\rho/c_{66})^{1/2}$

(9) $\left(\dfrac{4\rho}{c_{11}+c_{22}+2c_{66}+\sqrt{(c_{11}-c_{22})^2+4(c_{12}+c_{66})^2}}\right)^{1/2}$

FIGURE 3.16. **Orthorhombic. Propagation in the XY plane. Curves are for barium sodium niobate, with the piezoelectric effect neglected.**

For propagation in the XZ plane the pure shear wave is polarized along the Y axis,

$$\left(\frac{k}{\omega}\right)_2 = \rho^{1/2}\{c_{66}\sin^2\theta + c_{44}\cos^2\theta\}^{-1/2}. \tag{3.37}$$

The quasishear wave is

$$\left(\frac{k}{\omega}\right)_1 = (2\rho)^{1/2}\left\{c_{55} + c_{11}\sin^2\theta + c_{33}\cos^2\theta - \sqrt{(c_{55} + c_{11}\sin^2\theta + c_{33}\cos^2\theta)^2 - 4\bar{C}}\right\}^{-1/2} \tag{3.38}$$

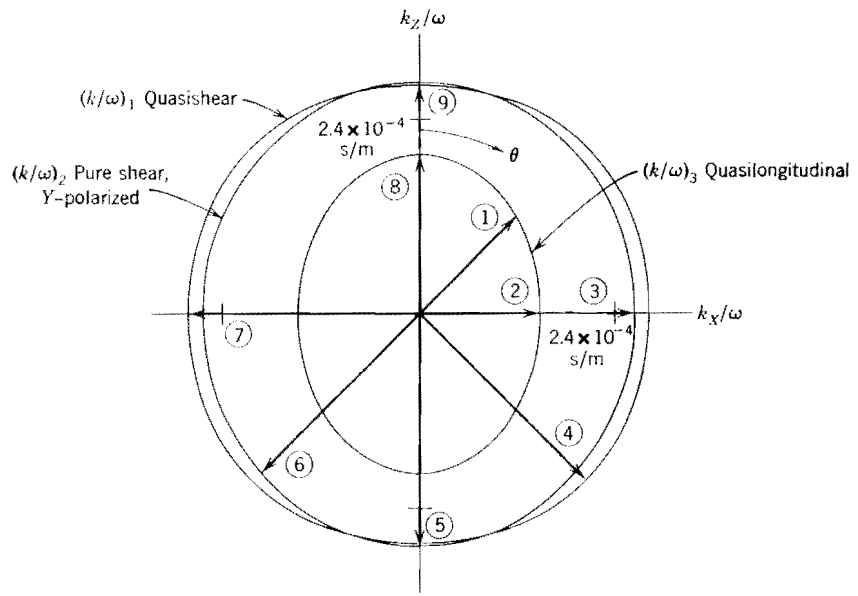

(1) $\left(\dfrac{4\rho}{c_{11} + c_{33} + 2c_{55} + \sqrt{(c_{11} - c_{33})^2 + 4(c_{13} + c_{55})^2}}\right)^{1/2}$

(2) $(\rho/c_{11})^{1/2}$ (3) $(\rho/c_{66})^{1/2}$

(4) $\left(\dfrac{4\rho}{c_{11} + c_{33} + 2c_{55} - \sqrt{(c_{11} - c_{33})^2 + 4(c_{13} + c_{55})^2}}\right)^{1/2}$

(5) $(\rho/c_{44})^{1/2}$ (6) $\left(\dfrac{2\rho}{c_{44} + c_{66}}\right)^{1/2}$

(7)(9) $(\rho/c_{55})^{1/2}$ (8) $(\rho/c_{33})^{1/2}$

FIGURE 3.17. **Orthorhombic. Propagation in the XZ plane. Curves are for barium sodium niobate, with the piezoelectric effect neglected.**

and the quasilongitudinal wave is

$$\left(\frac{k}{\omega}\right)_3 = (2\rho)^{1/2}\left\{c_{55} + c_{11}\sin^2\theta + c_{33}\cos^2\theta + \sqrt{(c_{55} + c_{11}\sin^2\theta + c_{33}\cos^2\theta)^2 - 4\bar{C}}\right\}^{-1/2}. \tag{3.39}$$

where

$$\bar{C} = (c_{11}\sin^2\theta + c_{55}\cos^2\theta)(c_{55}\sin^2\theta + c_{33}\cos^2\theta) - (c_{13} + c_{55})^2\sin^2\theta\cos^2\theta.$$

Curves are shown in Fig 3.17.

In the YZ plane the pure shear wave is polarized along the X axis

$$\left(\frac{k}{\omega}\right)_1 = \rho^{1/2}\{c_{66}\sin^2\theta + c_{55}\cos^2\theta\}^{-1/2}. \tag{3.40}$$

The quasishear wave is

$$\left(\frac{k}{\omega}\right)_2 = (2\rho)^{1/2}\left\{c_{44} + c_{22}\sin^2\theta + c_{33}\cos^2\theta - \sqrt{(c_{44} + c_{22}\sin^2\theta + c_{33}\cos^2\theta)^2 - 4C}\right\}^{-1/2} \tag{3.41}$$

and the quasilongitudinal wave is

$$\left(\frac{k}{\omega}\right)_3 = (2\rho)^{1/2}\left\{c_{44} + c_{22}\sin^2\theta + c_{33}\cos^2\theta + \sqrt{(c_{44} + c_{22}\sin^2\theta + c_{33}\cos^2\theta)^2 - 4C}\right\}^{1/2}, \tag{3.42}$$

where

$$C = (c_{22}\sin^2\theta + c_{44}\cos^2\theta)(c_{44}\sin^2\theta + c_{33}\cos^2\theta) - (c_{23} + c_{44})^2\sin^2\theta\cos^2\theta.$$

Curves are shown in Fig. 3.18.

C. PURE MODE DIRECTIONS

In anisotropic media acoustic plane waves do not usually have particle motion polarized either parallel or normal to the wave vector. Pure longitudinal and pure transverse polarizations occur only for certain wave vector directions, called *pure mode directions*. These may occur in both symmetry and nonsymmetry directions.

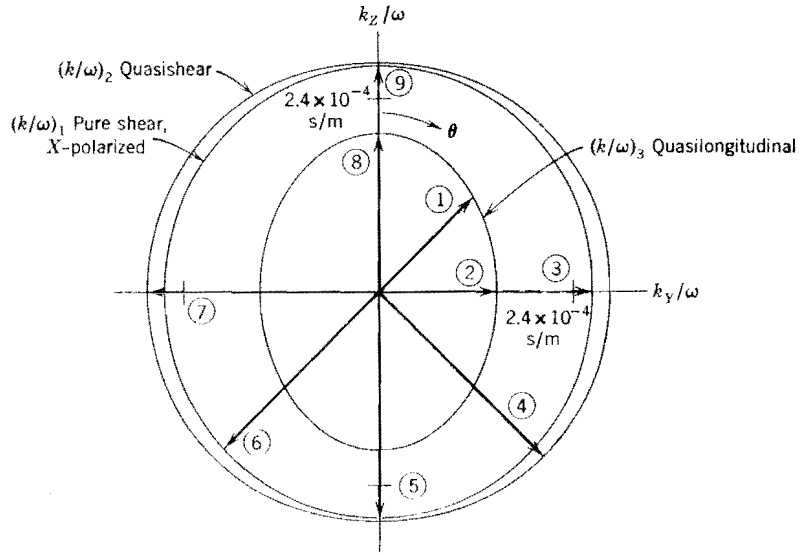

(1) $\left(\dfrac{4\rho}{c_{22}+c_{33}+2c_{44}+\sqrt{(c_{22}-c_{33})^2+4(c_{23}+c_{44})^2}}\right)^{1/2}$

(2) $(\rho/c_{22})^{1/2}$

(3) $(\rho/c_{66})^{1/2}$

(4) $\left(\dfrac{4\rho}{c_{22}+c_{33}+2c_{44}-\sqrt{(c_{22}-c_{33})^2+4(c_{23}+c_{44})^2}}\right)^{1/2}$

(5) $(\rho/c_{44})^{1/2}$

(6) $\left(\dfrac{2\rho}{c_{55}+c_{66}}\right)^{1/2}$

(7) $(\rho/c_{44})^{1/2}$

(8) $(\rho/c_{33})^{1/2}$

(9) $(\rho/c_{55})^{1/2}$

FIGURE 3.18. **Orthorhombic. Propagation in the *YZ* plane. Curves are for barium sodium niobate, with the piezoelectric effect neglected.**

C.1 Symmetry Directions

Propagation in a Symmetry Plane

One pure shear mode, polarized normal to plane.

Propagation Normal to a 2-fold, 4-fold or 6-fold Axis

One pure shear mode, polarized parallel to axis.

Propagation Along A 2-fold Axis

All modes are pure.

Propagation Along a 3-fold, 4-fold or 6-fold Axis

All modes are pure.

Shear modes are degenerate.

C.2 Nonsymmetry Directions†

C.2a Hexagonal

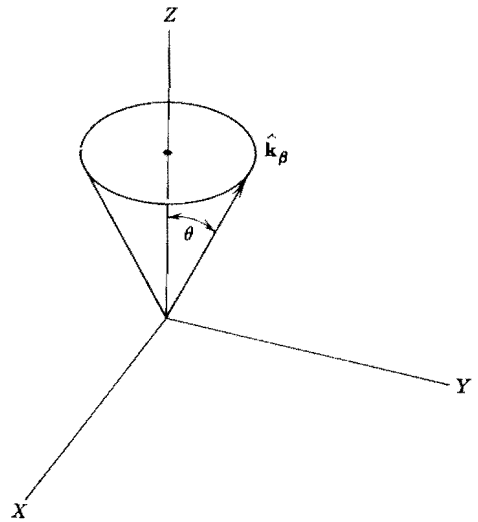

$$\cot^2\theta = \frac{c_{11}-2c_{44}-c_{13}}{c_{33}-2c_{44}-c_{13}}.$$

C.2b Trigonal (*32*, *3m*, $\bar{3}m$)

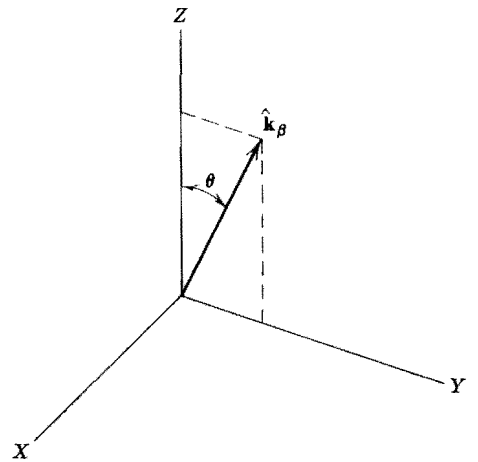

$$(c_{33}-2c_{44}-c_{13})\cot^3\theta + 3c_{14}\cot^2\theta - (c_{11}-2c_{44}-c_{13})\cot\theta - c_{14} = 0.$$

† After K. Brugger, "Pure Modes for Elastic Waves in Crystals," *J. Appl. Phys.* **36**, 759–768 (1965).

C.2c Trigonal (3, $\bar{3}$)

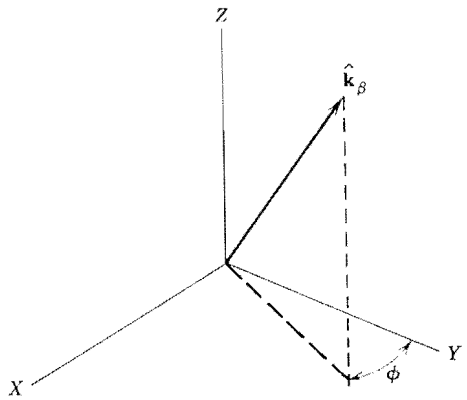

$$\tan 3\phi = -\frac{c_{25}}{c_{14}}$$

$$q = \frac{(\hat{k}_\beta)_Z}{(\hat{k}_\beta)_Y}$$

$$(c_{33} - 2c_{44} - c_{13})q^3 - \frac{3(\tan^2\phi + 1)^2}{(3\tan^2\phi - 1)}c_{14}q^2 - (\tan^2\phi + 1)(c_{11} - 2c_{44} - c_{13})q + \frac{(\tan^2\phi + 1)^3}{3\tan^2\phi - 1}c_{14} = 0.$$

C.2d Tetragonal ($4mm$, 422, $\bar{4}2m$, $4/mmm$)

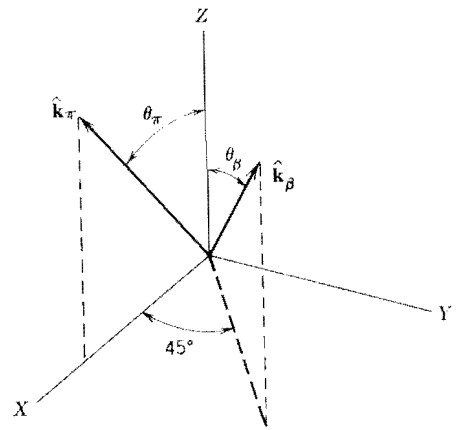

$$\cot\theta_\beta = \left\{\frac{c_{11} - 4c_{44} - 2(c_{13} - c_{66}) - c_{12}}{2(c_{33} - 2c_{44} - c_{13})}\right\}^{1/2}$$

$$\cot\theta_\pi = \left(\frac{c_{11} - 2c_{44} - c_{13}}{c_{33} - 2c_{44} - c_{13}}\right)^{1/2}.$$

C.2e Tetragonal (4, $\bar{4}$, $4/m$)

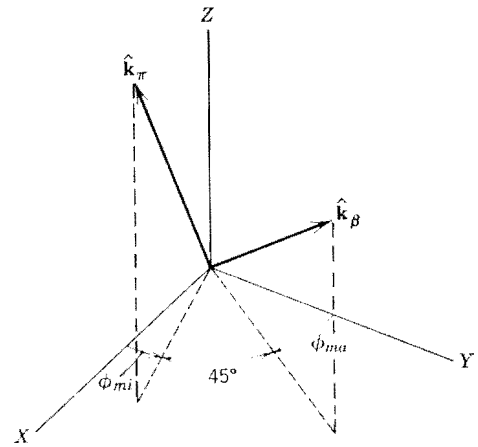

$$\tan 4\phi_{ma} = \frac{-4c_{16}}{c_{11} - c_{12} - 2c_{16}}$$

$$\phi_{mi} = \frac{\pi}{4} - \phi_{ma}.$$

$$\frac{(\hat{k}_\pi)_Z}{(\hat{k}_\pi)_X} = \left[\frac{\tan^2\phi_{mi} + 1}{c_{33} - 2c_{44} - c_{13}}\left\{c_{11} - 2c_{44} - c_{13} + \frac{(c_{11} - 2c_{66} - c_{12})2\tan^2\phi_{mi}}{\tan^4\phi_{mi} - 6\tan^2\phi_{mi} + 1}\right\}\right]^{1/2}.$$

$$\frac{(\hat{k}_\beta)_Z}{(\hat{k}_\beta)_X} = \left[\frac{\tan^2\phi_{ma} + 1}{c_{33} - 2c_{44} - c_{13}}\left\{c_{11} - 2c_{44} - c_{13} + \frac{(c_{11} - 2c_{66} - c_{12})2\tan^2\phi_{ma}}{\tan^4\phi_{ma} - 6\tan^2\phi_{ma} + 1}\right\}\right]^{1/2}.$$

Note that ϕ_{ma} and ϕ_{mi} are the same as (8) and (9) in Fig. 3.13.

C.2f Orthorhombic

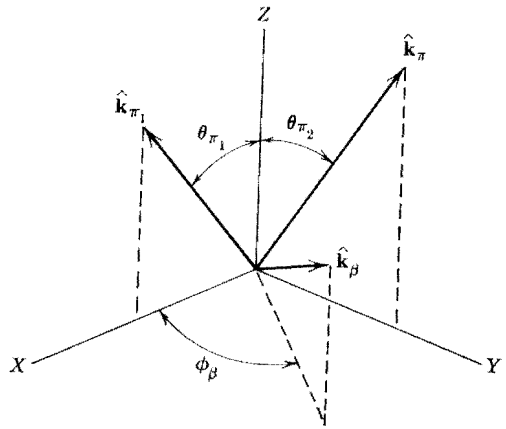

$$\cot \theta_{\pi_1} = \left(\frac{c_{11} - 2c_{55} - c_{13}}{c_{33} - 2c_{55} - c_{13}}\right)^{1/2}$$

$$\cot \theta_{\pi_2} = \left(\frac{c_{22} - 2c_{44} - c_{23}}{c_{33} - 2c_{44} - c_{23}}\right)^{1/2}$$

$$\tan \phi_\beta = \left\{\frac{A_1(C_1 - C_2) - B_1C_1}{A_2(C_2 - C_1) - B_2C_2}\right\}^{1/2} \qquad \frac{(\hat{k}_\beta)_Z}{(\hat{k}_\beta)_X} = \left\{\frac{B_2(B_1 - A_1) - A_2B_1}{A_2(C_2 - C_1) - B_2C_2}\right\}^{1/2}$$

$$A_1 = c_{11} - 2c_{55} - c_{13} \qquad B_1 = c_{11} - 2c_{66} - c_{12}$$

$$A_2 = c_{22} - 2c_{44} - c_{23} \qquad B_2 = c_{22} - 2c_{66} - c_{12}$$

$$C_1 = c_{33} - 2c_{55} - c_{13}$$

$$C_2 = c_{33} - 2c_{44} - c_{23}.$$